

Further Investigation for the SVD-based Analysis of Dynamical Noise on Chaos

Masaru Todoriki[†] and Shuichi Hasegawa[†]

[†]Graduate School of Engineering, The University of Tokyo
 7-3-1 Hongo, Bunkyo-ku, Tokyo 113-8656 Japan
 Email: todoriki@q.t.u-tokyo.ac.jp, hasegawa@q.t.u-tokyo.ac.jp

Abstract—We have already proposed a method to evaluate the influence of dynamical noise on chaotic systems [1]. It was demonstrated that the influence of dynamical noise on a typical chaotic system Chua's electronic circuit can be extracted by the temporal fluctuation of singular values (TFSV) obtained from singular value decomposition (SVD), independently of the presence of measurement noise. In this study, further investigation related to this method is performed regarding the influence of data length and embedding. As a result, it is found that an adequate data length can be determined by using a new index S and the characteristics in the both cases with embedding and without embedding are shown.

1. Introduction

Every physical system is subject to noise in the real world. In general, there are two types of noise in any physical system, namely, measurement noise and dynamical noise. Different from the former, the latter type of noise is said to be realistically intrinsic to a physical system and yields an extremely complicated mechanism accompanied by feedback. As a result, it is quite difficult to analyze both on the theoretical and experimental levels. On the other hand, since a chaos system displays particularly strong nonlinearity and sensitivity to its initial condition, dynamical noise may have a remarkable and fatal influence on a chaos system. Numerous studies concerning dynamical noise in chaos have appeared, such as estimation of noise levels [2], stabilization of the system such as stochastic resonance [3], vibrational resonance [4], coherence resonance [5, 6], and noise-induced stabilization [7, 8].

We have already proposed a method to evaluate the influence of dynamical noise on chaotic systems [1]. It was demonstrated that the influence of dynamical noise on a typical chaotic system Chua's electronic circuit can be extracted by the temporal fluctuation of singular values (TFSV) obtained from singular value decomposition (SVD), independently of the presence of measurement noise. In this study, further investigation related to this method is performed regarding the influence of data length and embedding.

2. Proposed Method

2.1. Noise

Generally, dynamical noise and measurement noise are defined for a flow system, respectively, as follows:

$$\dot{\mathbf{x}} = \mathbf{f}(\mathbf{x}, \xi^{(D)}), \quad (1)$$

$$\mathbf{y} = \mathbf{g}(\mathbf{x}) + \xi^{(M)}, \quad (2)$$

where \mathbf{x} and \mathbf{y} are, respectively, the underlying state vector and the observed one; \mathbf{f} is a governing function of the system; \mathbf{g} is an observation function; and $\xi^{(D)}$ and $\xi^{(M)}$ are dynamical and measurement noise, respectively.

2.2. Temporal Fluctuation of Singular Values (TFSV)

SVD is the operation to diagonalize the singular matrix. Now, if the $N \times n$ rectangular matrix X is diagonalized, the covariance matrix $X^t X$ can be decomposed into $X^t X = V \Sigma^2 V^t$, where Σ^2 is the $n \times n$ diagonal matrix and V and V^t are the $n \times n$ orthogonal matrix and the transposed matrix of V , respectively. Here, $V V^t = V^t V = I_n$ is satisfied using the $n \times n$ unit matrix I_n . As $\Sigma^2 = \text{diag}(\sigma^2(1), \sigma^2(2), \dots, \sigma^2(n))$ is obtained, we can extract singular values (SVs) $\{\sigma(i) | i = 1, 2, \dots, n\}$, which are non-zero. The relatively larger SVs correspond to the principal orthogonal basis of the deterministic system. In general, measured data is frequently obtained as a scalar time series. The procedure of SVD for such data is explained. Now, a (n, J) -window: $\{v_i, v_{i+J}, \dots, v_{i+(n-1)J}\}$ is prepared, where n is the number of elements of the window and J is a sample time in applying the method of delays as described in Ref.[9]. Here, a finite measured time series $\{v_i \in R | i = 1, 2, \dots, N+n-1\}$ is transformed into the $N \times n (N \gg n)$ matrix X and the $n \times n$ covariance matrix $X^t X$ can be obtained.

2.3. In the presence of Measurement Noise

In the presence of measurement noise, each SV uniformly increases, since the underlying state vectors and the noise are uncorrelated, as explained in Ref.[9]. Namely, the covariance matrix $X^t X$ has a quite simple structure that is almost diagonal, where all diagonal values are larger by the same amount than those of a noiseless case. If the system remains steady, such diagonal values are expected to be nearly constant independent of the passage of time.

2.4. In the presence of Dynamical Noise

On the other hand, in the presence of dynamical noise, the result is utterly different from the case of measurement noise and $X^T X$ loses its simple structure. Since the underlying state vectors and dynamical noise are correlated, the dynamical noise complicatedly affects both each diagonal component and each off-diagonal component. The operation of SVD is to reduce the values of all of off-diagonal components by means of a similarity transformation of the orthogonal matrix. Accordingly, in the process of SVD, the complexity of the components spreads on diagonal components and, therefore, each value of diagonal components complicatedly changes. Moreover, since the statistical properties of both components depend upon the time series data, from which $X^T X$ is built, SVs temporally fluctuate for consecutive time series. Thus, the influence of dynamical noise on chaos can be extracted with a different form from that of measurement noise. This result means that the influences of dynamical noise and measurement noise can be distinguished even in the case of the noise-mixed data composed of both noises. The concrete way of extracting TFSV is explained next.

2.5. Performance Index S

In practice, TFSV can be estimated as follows (see Fig.1). First, temporally consecutive time series data sets are prepared. Each of sets is called an “interval” $\{I_k | k = 1, 2, \dots, N_{int}\}$ in this paper. In each I_k , N elements are included such as $\{v_{N(k-1)}, v_{N(k-1)+1}, \dots, v_{N(k-1)+N}\}$. Second, SVs $\{\sigma_k(i) | i = 1, 2, \dots, n\}$ are calculated in each I_k , where i is an “Index” of SVs lined in descending order. Third, each standard deviation $S(i)$ of SVs over all *interval* is calculated every i th Index. At last, as an averaged $S(i)$, S_{av} is obtained as concrete expression of TFSV, as follows.

$$S(i) = \sqrt{\frac{\sum_{k=1}^{N_{int}} (\sigma_k(i) - \overline{\sigma(i)})^2}{N_{int}}}, \quad (3)$$

$$S_{av} = \frac{\sum_{i=1}^n S(i)}{n}, \quad (4)$$

where $\overline{\sigma(i)}$ is the averages of $\sigma_k(i)$ for all Index at i th Index and $S(i), S_{av} \in [0, \infty]$.

In the previous work, we introduced an original performance index: correlation coefficient C . While, in this study, the new index S is induced instead of C . The new index can bring us some advantages regarding normalization of data length, comprehensibility, and so on. As C has been already normalized by variance of data to the range of $[-1, 1]$, therefore, there is no reasonable way for further normalization. Moreover, C has a difficult concept to understand the meaning compared with S .

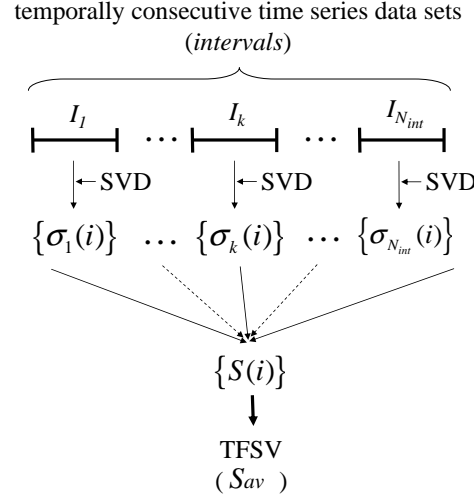


Figure 1: The concept of the extraction of TFSV. Temporally consecutive time series data sets are prepared. Each of sets is called an “interval” $\{I_k | k = 1, 2, \dots, N_{int}\}$. N elements; $\{v_{N(k-1)}, v_{N(k-1)+1}, \dots, v_{N(k-1)+N}\}$ are included in each I_k . Meanwhile, each performance index $S(i)$ of SVs over all *interval* is calculated for every i th Index. TFSV can be estimated by the average S_{av} as a proxy of $S(i)$.

3. Numerical Analysis

3.1. Preparation

Chua’s electronic circuit is used as a typical chaos system, which is described by the 3-dimensional ordinary differential equations that follow [10],

$$C_1 \frac{dV_{C_1}}{dt} = \frac{1}{R}(V_{C_2} - V_{C_1}) - f_{N_R}(V_{C_1}), \quad (5)$$

$$C_2 \frac{dV_{C_2}}{dt} = \frac{1}{R}(V_{C_1} - V_{C_2}) + i_L, \quad (6)$$

$$L \frac{di_L}{dt} = -V_{C_2}, \quad (7)$$

where $f_{N_R}(V_{C_1}) = G_b V_{C_1} + \frac{1}{2}(G_a - G_b)|V_{C_1} + B_p| - |V_{C_1} - B_p|$. V_{C_1} , V_{C_2} and i_L indicate voltage of two capacitors C_1 , C_2 and the current of coil L , respectively. $f_{N_R}(V_{C_1})$ denotes the 3-segment odd-symmetric voltage-current characteristic of the nonlinear resistor N_R , by which the system exhibits a large variety of typical chaotic behaviors. The *i.i.d.* dynamical noise ξ with a 0 mean is added to V_{C_1} such as $V_{C_1} \rightarrow V_{C_1} + \xi$ as additive noise. In this work values of parameters giving rise to double-scroll chaos are selected as follows, $C_1 = 10 \text{ nF}$, $C_2 = 100 \text{ nF}$, $L = 18 \text{ mH}$, $1/R = 0.55 \text{ 1}/\Omega$, $G_a = -0.758 \text{ mA}/V$, $G_b = -0.409 \text{ mA}/V$, and $B_p = 1.17 \text{ V}$. Here, the analyses are performed for the scalar time series of V_{C_1} . In this study, 4 kinds of time series are prepared, these being noise-free data (*NF-data*), measurement noise data (*M-data*), dynamical noise data (*D-data*), and noise-mixed data composed of both dynamical

ical noise and measurement noise (*DM-data*). Each noise level is given as a ratio of a standard deviation of noise data to that of the time series V_{C_1} in *NF-data*. The range of the noise amplitude is 0.01%-20.0% for *M-data* and 0.01%-3.7% for *D-data*, where 3.7% is the maximum, below which a chaotic state can be retained. For *DM-data*, measurement noise with a 20.0% noise level is added to all *D-data*. The 4th-order Runge-Kutta method is used with a constant time step $\tau_s = 0.000005$. The number of elements N in each interval and the number of intervals N_{int} are 100,000 and 10,000, respectively. SVD is performed for all intervals to extract TFSV. However, ahead of SVD, an adequate (n, J) window should be determined, satisfying the window length $\tau_w = n\tau_L = nJ\tau_s$, where the lag time τ_L is expressed as $\tau_L = J\tau_s$. In particular, the most important parameter is τ_w . Though the detail is not presented here, in this case, $\tau_w = 60\tau_s$ can be determined by considering the band-limiting frequency in FFT analysis as explained in [9]. However, there are some difficulties in deciding the properties of the adequate window. Here, the result should satisfy $nJ = 60$. In this paper, SVD is undertaken for the two cases: $(n, J) = (4, 15)$ and $(3, 20)$.

3.2. Results of TFSV

Figure 2 shows results of TFSV for the 4 representatives. In (a) the results of a performance index C_{av} are illustrated in the previous work for comparison with the new index S_{av} . While, in (b) those of the new index S_{av} are shown. In both cases, a window condition $(4, 15)$ is adopted for embedding. From figure 2, quite similar tendencies between the results of C_{av} and S_{av} can be seen, though the direction of the increase of TFSV is opposite. Accordingly, it can be said that S_{av} is effective for extraction of TFSV.

4. Estimation of Data Length N in each Interval

The influence of the data length in each *interval* on S_{av} is estimated. The estimation is carried out by using normalized S_{av} , that is, $\overline{S_{av}}$, which is normalized by multiplying \sqrt{N} , where N is the number of data points in each *interval*. The result can be shown in figure 3. The data length from 1,000 to 100,000 are used for this estimation. According to figure 3, as the data length increases, the curve of $\overline{S_{av}}$ converges in the data length more than 30,000 points approximately. It can be said that the data length 100,000, which is used in this study, is statistically sufficient.

5. Estimation of Embedding

The influence of embedding is recognized here. We prepare two cases; the embedding case and the no-embedding one. In the embedding case, the window condition $(n, J) = (3, 20)$ is adopted. Therefore, a set $\{v_i, v_{i+20}, v_{i+2 \times 20}\}$ for i th row components of the matrix X is used and TFSV is calculated. On the other hand, in the no-embedding case, a

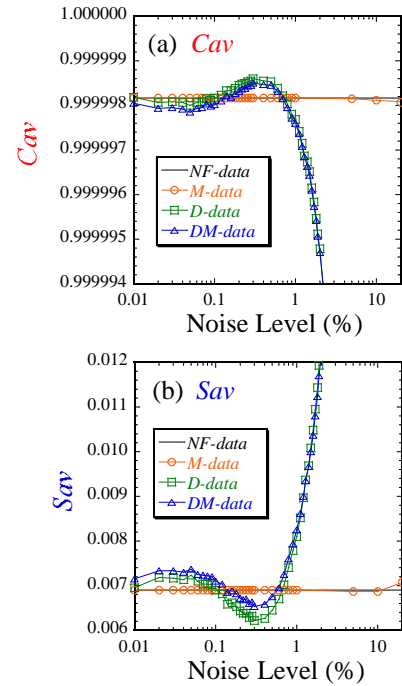


Figure 2: Results of TFSV for the 4 representatives. In (a) the results of a performance index C_{av} are illustrated in the previous work. In (b) those of the new index S_{av} are shown. In both cases, a window condition $(4, 15)$ is adopted for embedding. Both results indicate quite similar tendencies each other, though the direction of the increase of TFSV is opposite.

set composed of three i th variables $\{Vc1_i, Vc2_i, iL_i\}$ for i th row ones is directly used for X . Figure 4 shows the results. The results of the both cases are compared for each case of S_{av} , $S(1)$, $S(2)$, and $S(3)$, respectively. In S_{av} , regarding the influence of dynamical noise, the range of the values S in the embedding case is larger than in the no-embedding one. This means that the analysis in the embedding case can much more sensitively extract the influence of dynamical noise than that in the no-embedding one. Besides, in the embedding case, the influence of measurement noise can be avoided more effectively than in the no-embedding case, because uncorrelated signals of measurement noise can be canceled in the course of SVD in the embedding case differently from the no-embedding one.

6. Conclusions

Further investigation related to the proposed method is performed. The new performance index S is induced. Some advantages are obtained and, in particular, the analysis of the influence of data length becomes possible through normalization. As the results, it is found out that the data length 100,000 in each *interval* adopted in our analysis is statistically sufficient. In the estimate of embedding, the

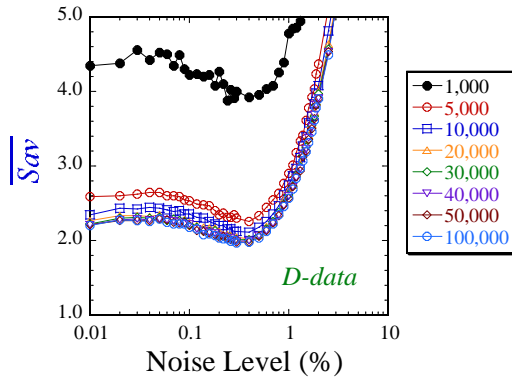


Figure 3: Influence of the data length in each *interval*. \overline{S}_{av} is normalized by multiplying \sqrt{N} , where N is the number of data points in each *interval*. As data length increases, the curve of \overline{S}_{av} converges.

characteristic concerning dynamical noise and measurement one are indicated, respectively.

Acknowledgments

We would like to thank Professor K. Aihara and his colleagues, Professor T. Ikeguchi, and Professor M. Adachi for fruitful comments and stimulating discussion. This study was supported by a Grant-in-Aid for Scientific Research of JSPS.

References

- [1] M. Todoriki, H. Nagayoshi, and A. Suzuki, Temporal Fluctuation of Singular Values caused by Dynamical Noise in Chaos, *Phys. Rev. E*, **72**, pp. 036207, 2005.
- [2] J. P. M. Heald, and J. Stark, Estimation of Noise Levels for Models of Chaotic Dynamical Systems, *Phys. Rev. Lett.*, **84-11**, pp. 2366, 2000.
- [3] L. Gammaitoni, P. Hänggi, P. Jung, and F. Marchesoni, Stochastic Resonance, *Rev. Mod. Phys.*, **70-1**, pp. 223, 1998.
- [4] P. S. Landa, and P. V. E. McClintock, Vibrational Resonance, *J. Phys. A: Math. Gen.*, **33**, pp. L433, 2000.
- [5] E. I. Volkov, M. N. Stolyarov, A. A. Zaikin, and J. Kurths, Coherence Resonance and Polymodality in Inhibitory Coupled Excitable Oscillators, *Phys. Rev. E*, **67**, pp. 066202, 2003.
- [6] R. Morse, and A. Longtin. Coherence and Stochastic Resonance in threshold crossing Detectors with Delayed FeedBack, *Phys. Lett. A*, **359**, pp. 640, 2006.
- [7] R. Wackerbauer, When Noise Decreases Deterministic Diffusion, *Phys. Rev. E.*, **59-3**, pp. 2872, 1999.

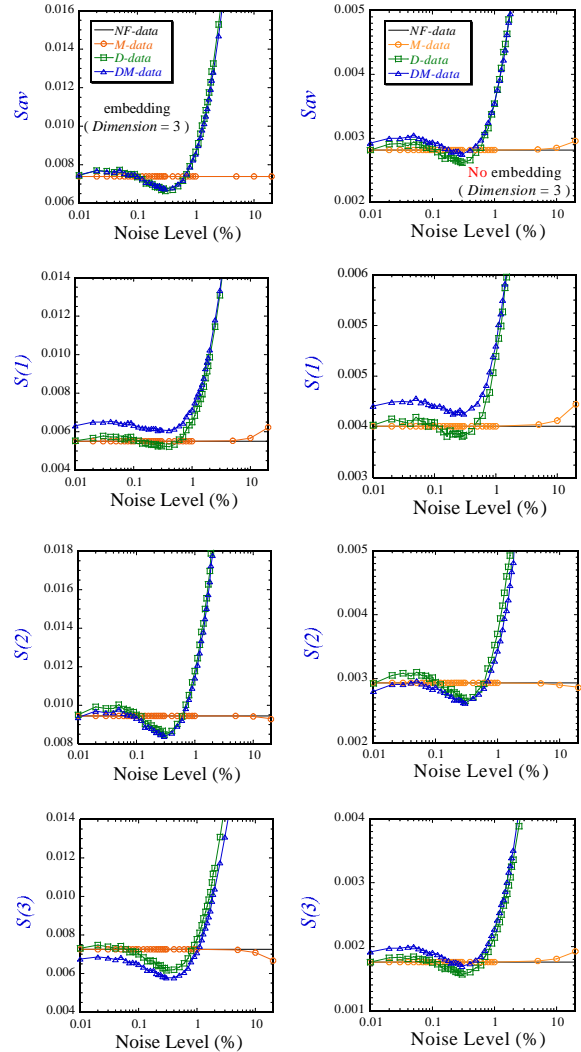


Figure 4: The comparison between the results of the embedding case (on the left-hand side) and the no-embedding case (on the right-hand side). The comparison is carried out in each case of S_{av} , $S(1)$, $S(2)$, and $S(3)$.

- [8] J. B. Gao., J. Hu, W. W. Tung, and Y. H. Cao Distinguishing chaos from noise by scale-dependent Lyapunov exponent, *Phys. Rev. E*, **74**, pp. 066204, 2006.
- [9] D. S. Broomhead, and G. P. King, Extracting Qualitative Dynamics from Experimental Data, *Physica D*, **20**, pp. 217, 1986.
- [10] R. N. Madan, Chua's Circuit: A Paradigm for Chaos, *World Scientific Nonlinear Science Ser. B*, World Scientific vol.1, 1993.